



## Article

# Framework for Monitoring the Spatiotemporal Distribution and Clustering of Drought Characteristics in Hunan Province

Chunxiao Huang <sup>1</sup>, Shunshi Hu <sup>1,2,\*</sup>, Muhammad Hasan Ali Baig <sup>3</sup> and Ying Huang <sup>1</sup>

<sup>1</sup> School of Geographical Sciences, Hunan Normal University, Changsha 410081, China; hcx@smail.hunnu.edu.cn (C.H.); ying.huang@hunnu.edu.cn (Y.H.)

<sup>2</sup> Key Laboratory of Geospatial Big Data Mining and Application, Changsha 410081, China

<sup>3</sup> Institute of Geo-Information and Earth Observation, Arid Agriculture University Rawalpindi, Rawalpindi 46300, Pakistan; mhasanbaig@uaar.edu.pk

\* Correspondence: shunshi.hu@hunnu.edu.cn

**Abstract:** Drought is a widespread phenomenon in the context of global climate change. Owing to the geographical location of Hunan Province in the middle reaches of Yangtze River and the abundance of forests area in this region with a large population, there is a need to focus on the impacts of drought for devising policies. The spatiotemporal distribution scheme of a given area must be determined to plan water management and protect ecosystems effectively. This study proposes a framework for exploring the spatiotemporal distribution model of drought using comprehensive surveys of historical meteorological stations, which consists of two parts, namely the characteristics of drought extraction in the spatiotemporal distribution and drought models discovered by the clustering method. Firstly, we utilized the run theory to extract drought characteristics, such as drought duration, drought severity, and drought intensity. Secondly, the K-means clustering method was adopted to explore the distribution patterns on the basis of the drought characteristics. Lastly, the method was applied to Hunan Province. Results show that historical drought conditions can be monitored with their characteristics of spatiotemporal variability. Three drought distribution clusters exist in this region. Cluster 1 in western Hunan tends to be a long-term, low-intensity drought, cluster 2 in the southern part tends to be a short-term, high-intensity drought, and cluster 3 in the central part is prone to severe drought. The proposed framework is flexible as it allows parameters to be adjusted and extraction methods to achieve reasonable results for a given area.

**Keywords:** drought; spatiotemporal distribution; drought characteristics; SPEI; Hunan Province



**Citation:** Huang, C.; Hu, S.; Ali Baig, M.H.; Huang, Y. Framework for Monitoring the Spatiotemporal Distribution and Clustering of Drought Characteristics in Hunan Province. *Appl. Sci.* **2021**, *11*, 11524. <https://doi.org/10.3390/app112311524>

Academic Editors: Stefania Pindozi and Francesco Fiorillo

Received: 18 September 2021

Accepted: 27 November 2021

Published: 5 December 2021

**Publisher's Note:** MDPI stays neutral with regard to jurisdictional claims in published maps and institutional affiliations.



**Copyright:** © 2021 by the authors. Licensee MDPI, Basel, Switzerland. This article is an open access article distributed under the terms and conditions of the Creative Commons Attribution (CC BY) license (<https://creativecommons.org/licenses/by/4.0/>).

## 1. Introduction

Droughts, which last for several days or even years, are complex and recurring natural phenomena [1]. Their formation is mainly due to a substantial decline in water availability caused by insufficient precipitation [2,3]. Global warming and climate change exacerbate droughts [4,5]. Severe and persistent droughts can lead to ecological disasters [6] and pose serious risks to normal human life. A report shows that approximately 800,000 people died from droughts worldwide between 1970 and 2017 [7]. Effective spatiotemporal assessment of droughts can provide ecological knowledge and help in reducing the impact of drought. It is conducive to regional water resource management and decision-making with regard to ecological water use planning and ultimately alleviates the drought situation and reduces economic losses [8].

Meteorological station recordings and remote sensing data are two widely used data sources for drought-related research over the past decades [9–13]. Remote sensing data present many advantages when used for large areas that lack meteorological stations. However, several uncertainties due to algorithms based on derived products from satellite imagery [14,15] and cloud contamination [16] limit the accuracy of such data. For example, precipitation products from remote sensing mainly rely on passive microwave or

infrared technologies [17,18], which are likely to be affected by topography and thus induce uncertainties in data quality. In addition, remote sensing precipitation products usually have a coarser spatial resolution; for example, the Tropical Rainfall Measuring Mission (TRMM) and the Climate Precipitation Center's morphing technique precipitation product have a spatial resolution of  $0.25^\circ$  [19], which is unsuitable for revealing the details of spatial heterogeneity in a given region. Therefore, using meteorological station recordings to monitor drought status has become a popular method, especially for mountain areas with heavy clouds or rainy weather. Furthermore, meteorological stations usually have long historical records and can establish a long-term drought parameter sequence, which is useful for exploring drought characteristics.

Hydrological and statistical models have been established for drought monitoring and climate response analysis. Wavelet analysis [8,20], the soil and water assessment tool (SWAT), the run theory [21], and cluster analysis [2] are commonly used models for monitoring drought. Amongst them, SWAT is currently the most widely used hydrological model. It uses elevation data to divide a watershed into sub-units, which are composed of all areas with similar landscape characteristics [22]. Combining SWAT with the drought index is found useful in investigating the impact of climate on future and past droughts in multiple regions [23]. However, the data input format of soil and water assessment tools to be used in these models have the restriction of a specific format, besides the requirement of data in days and the need for real data for the sake of verification, which makes this approach inconvenient to use. Wavelet analysis is a statistical model that explores the changes in drought over time by acquiring spectrograms. For time series with unequal intervals, least-squares wavelet analysis [24] and least-squares cross wavelet analysis [8] are applied in drought monitoring based on the drought indices.

Using drought indices derived from the meteorological station observations to monitor drought situations has a long history and is proven to be effective in exploring drought spatiotemporal distribution patterns [2,3,25]. In the past decades, scientists have developed many drought indices by utilizing meteorological station recordings; examples include the precipitation condition index (PCI) [26], temperature condition index (TCI) [27], standardized precipitation index (SPI) [28], and standardized precipitation evapotranspiration index (SPEI) [29]. Amongst these drought indices, SPEI is the most sophisticated and widely used tool because it is designed to consider both precipitation and potential evapotranspiration (PET) while determining drought, and it can capture multi-temporal characteristics of drought [3,12]. When considering a given drought event, scientists usually focus on several quantified characteristics of the drought, such as duration, severity, and intensity [30]. However, as the SPEI index cannot directly and quantitatively describe the characteristics of drought events, there is a need to use other techniques along with SPEI.

By defining multiple thresholds, the run-theory [21] method can be used as a powerful tool to distinguish drought and non-drought statuses and extract drought characteristics from drought indices [31]. For example, Sun et al. [32] proposed a method for urban drought disaster risk analysis and assessment by integrating the run theory, the copula function, the crop growth model, and natural disaster risk assessment technology. Malik et al. [33] classified droughts using the run theory and reported that the probability of occurrence of moderate drought events is relatively higher than that of severe and extreme drought events in Uttarakhand (India). He et al. [31] used the run theory to identify the frequency, duration, severity, and intensity of all droughts in China on the basis of the monthly percentage of the precipitation anomaly rate index and found that China has five obvious meteorological drought-prone areas. These studies have shown that the run theory method can effectively identify and detect the temporal characteristics of drought [34,35]. Hence, determining whether the run theory can effectively and efficiently detect temporal drought features from SPEI sequences is an interesting topic.

With regard to the spatial distribution of drought characteristics, drought cluster analysis methods are widely used to identify homogeneous regions with similar drought characteristics. These methods include fuzzy c-means [5], quantile regression [2], and

K-means. Drought indices, such as PCI, TCI, SPI, and SPEI, are normally set as input data for these cluster analysis methods to detect the spatial distribution of drought characteristics [2,5,25,36–38]. Shiau et al. [2] utilized the hierarchical agglomerative clustering algorithm to analyze the different quantile slopes of SPI-3 at 12 stations in Taiwan, and the results showed that stations along the east coast were likely to be severely affected. Xie et al. [37] used k-means clustering to divide Xinjiang's drought spatial distribution patterns into three clusters on the basis of SPI. By using the standardized precipitation temperature index as a feature, Ali et al. [38] partitioned the 52 meteorological stations in Pakistan into nine clusters. However, despite reflecting the statuses of drought and wetness, these drought index values were used directly in cluster analysis methods, which might be inappropriate for effectively distinguishing the two statuses. Introducing quantitative characteristics that indicate the degree and severity of drought may be a better option for describing drought in spatial and temporal aspects.

In this study, we developed a method to identify the spatiotemporal distribution of drought characteristics on the basis of meteorological station records in Hunan Province, China, which is a major grain-producing area and is often affected by floods and droughts [39]. This method consists of two steps. Firstly, it is designed to derive drought characteristics, including drought duration, severity, and intensity, from the SPEI index, by integrating the run-theory method. Secondly, drought spatial distribution patterns are derived by clustering drought characteristics via the K-means cluster method. Hunan Province is located in a subtropical region with relatively abundant rainfall, but it is still susceptible to seasonal drought events. According to historical statistics, the average drought in Hunan Province is about 701,000 hm<sup>2</sup>/year, of which the catastrophic drought area accounts for approximately 324,000 hm<sup>2</sup> [40]. Therefore, studying the drought characteristics of Hunan Province from spatial and temporal aspects is meaningful for ecological protection, regional water supply, and agricultural planning.

The rest of the paper is organized as follows. Section 2 presents an overview of the study area and the dataset used. Section 3 describes the research method in detail. Section 4 demonstrates the spatiotemporal distribution and drought characteristics of homogeneous regional stations in Hunan Province. Sections 5 and 6 provide the discussion and conclusions, respectively.

## 2. Study Area and Dataset

Hunan Province (108°47'–114°15' E and 24°38'–30°08' N) (Figure 1) is situated in the middle reaches of Yangtze River in China. It is surrounded by mountains in the east, south, and west; the central hills are undulating, and the northern lake basin is flat. The northeast opening presents an asymmetrical horseshoe-shaped basin, with four rivers running through the territory (Figure 1b) [41]. The study area has a subtropical monsoon climate, with an annual average temperature of about 16 °C–18 °C and annual rainfall of 1300–1600 mm [39].

Hunan Province has a total of 97 meteorological stations. The corresponding daily precipitation and temperature data between 1965 and 2015 were downloaded from the Hunan Meteorological Bureau. The meteorological recordings had several missing and abnormal values that needed to be removed and processed. In the end, 88 meteorological station recordings (Figure 1a) were retained to calculate the monthly average temperature and cumulative monthly precipitation.

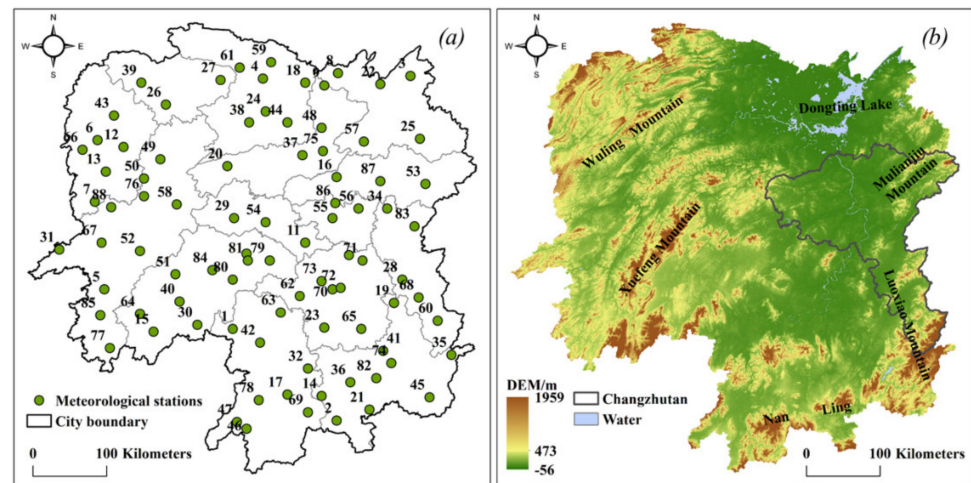


**Figure 1.** Meteorological stations and topography in Hunan Province: (a) Meteorological stations distribution, (b) topography and mountain distribution.

### 3. Methodology

The methodology adopted in this study consisted of two parts (Figure 2). The first part was used to extract drought temporal features by integrating the run theory with the SPEI drought index. The second part was implemented to derive drought spatial patterns by clustering drought characteristics and the latitude and longitude properties of the meteorological stations. The details of Parts 1 and 2 are presented in Sections 3.1 and 3.2, respectively.

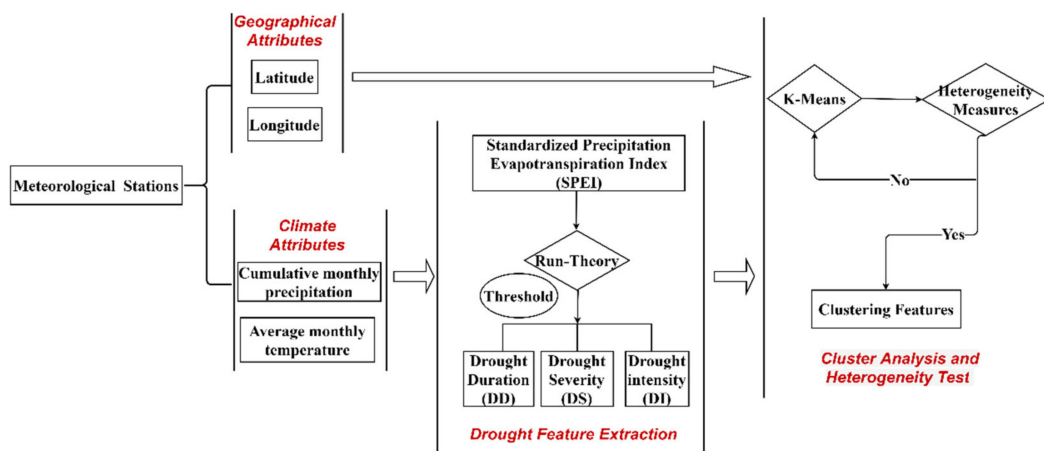


**Figure 2.** Flowchart of detecting drought spatiotemporal characteristics.

#### 3.1. Extraction of Drought Characteristics

As a powerful tool for describing the characteristics of meteorological drought, the SPEI drought index can obtain the time stamp and intensity of drought at multiple time scales; hence, it has widely been used in drought monitoring communities [3,9]. By integrating the run-theory with the SPEI index with a one-month time scale (SPEI-1), several useful characteristics of drought events, such as drought duration, severity, and intensity, can be derived in detail to help in understanding the characteristics of consecutive drought events.

### 3.1.1. SPEI

SPEI [42] is calculated based on precipitation and potential evapotranspiration (*PET*). Its calculation proceeds in three main steps. Firstly, the monthly mean water balance *D* is calculated as follows [29]:

$$D = P - PET, \tag{1}$$

where *P* is the monthly precipitation (mm) and *PET* is the monthly potential evapotranspiration (mm) calculated with the Thornthwaite method [43].

The cumulative monthly mean water balance value ( $D_n^k$ ) at different time scales can be derived with Equation (2) [42]

$$D_n^k = \sum_{i=0}^{k-1} (P_{n-1-i} - PET_{n-1-i}), \tag{2}$$

where *k* is the cumulative number of months and *n* is the number of calculations.

Secondly, water balance is standardized using a logarithmic probability distribution function, such as *F(x)*. Thirdly, the SPEI index time series are calculated with Equation (3) [29]

$$\begin{aligned} SPEI &= w - \frac{c_0 + c_1w + c_2w^2}{1 + d_1w + d_2w^2 + d_3w^3} & P \leq 0.5, \\ SPEI &= -\left(\frac{c_0 + c_1w + c_2w^2}{1 + d_1w + d_2w^2 + d_3w^3}\right) & P > 0.5, P = 1 - P, \end{aligned} \tag{3}$$

where the probability weighted moment is  $w = \sqrt{-2\ln(P)}$  and the probability of exceeding a certain value is  $P = 1 - F(x)$ ; the other parameters are  $c_0 = 2.515517$ ,  $c_1 = 0.802853$ ,  $c_2 = 0.010328$ ,  $d_1 = 1.432788$ ,  $d_2 = 0.189269$ , and  $d_3 = 0.001308$ . If  $P > 0.5$ , then *P* should be replaced with  $1 - P$  because the sign of SPEI is reversed.

According to Bae and Musei et al. [3,7], SPEI index values represent the degree of drought or humidity; large SPEI values usually indicate moist or wet conditions, and small values generally represent dry situations. SPEI index values can be generally divided into different categories that represent the degree of drought or humidity by setting different thresholds, as shown in Table 1.

**Table 1.** Wet and dry status partitions based on SPEI.

SPEI Value	Wet/Dry Status
>2	Extremely wet
1.5 to 2	Severely wet
1 to 1.5	Moderately wet
0.5 to 1	Slightly wet
−0.5 to 0.5	Normal
−1 to −0.5	Mildly dry
−1.5 to −1	Moderately dry
−2 to −1.5	Severely dry
<−2	Extremely dry

### 3.1.2. Drought Characteristics

The run theory is a useful tool to extract drought characteristics, such as drought duration, drought severity and drought intensity, from a drought index; it was proposed by Yevjevich [21]. By setting appropriate thresholds to segment drought index time series, the run theory can identify the start and end times of a single drought event. Many characteristics can be used to describe a given drought event [7,35] by setting certain thresholds [7,44] on the basis of the drought index time series. For representativeness and simplicity, several classic drought characteristics were selected from previous studies. Their detailed definitions and formulations are shown in Table 2. The rules for determining these

drought characteristics from the SPEI-1 time series by using the run theory (Figure 3) are listed as follows [35]:

**Table 2.** Definitions and formulas of drought characteristics and several parameter settings in the applications of the run theory.

Drought Characteristics	Content	Formula (Value)
Drought Duration (DD)	Duration from the beginning to the end of the drought event	$DD = DD_b + DD_d + 1$ ( $DD = DD_e$ )
Drought Severity (DS)	Cumulative sum of the difference between the drought index value and its threshold during drought events	$DS = DS_b + DS_d$ ( $DS = DS_e$ )
Drought Intensity (DI)	Drought severity divided by respective drought duration	$DI = DD/DS$
$R_0$	Combined adjacent drought threshold	0
$R_1$	Drought occurrence threshold	-0.5
$R_2$	Identified individual drought practices with high severity	-1

$DD_b, DD_d, DD_e$  and  $DS_b, DS_d, DS_e$  represent the duration and the severity of drought events b, d, and e (Figure 3), respectively.

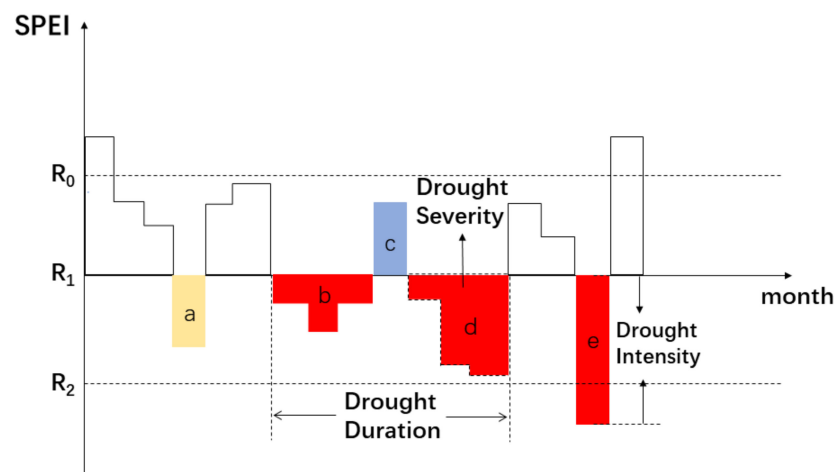


**Figure 3.** Identification of drought characteristics by the run theory.  $R_0$ ,  $R_1$ , and  $R_2$  are thresholds for combining adjacent drought, determining drought occurrence and identifying individual drought practices. a (brown color), c (sea-blue color) and b, d, and e (red color) represent normal, wet, and dry states, respectively.

- (1) If the values of SPEI-1 are less than  $R_1$ , they will be regarded as drought preliminary events (preliminary judgments), as shown in Figure 3, where a, b, d, and e denote four drought preliminary events.
- (2) If the length of a preliminary judgment is only one month and the corresponding SPEI-1 value is larger than  $R_2$ , it will be removed from the preliminary judgments. For example, in Figure 3, drought event a should be removed from preliminary judgments because it has a length of only one month.
- (3) If two consecutive drought events are separated only by a month interval and their corresponding SPEI-1 values are less than  $R_0$ , they can be merged as one drought event. In Figure 3, because drought events b and d are separated by c by only one month, b and d can be merged into one drought event.

The aforementioned rules were executed on each SPEI-1 index to derive the drought characteristics for corresponding meteorological stations.

### 3.2. Drought Spatial Distribution Pattern Identification

Using drought characteristics, extracted from meteorological station recordings to explore drought spatial distribution patterns, is important for drought hazard management, for which several cluster methods are generally used. Given that the unsupervised K-means method is relatively simple to implement and easily adapts to new examples, it was utilized in this study to explore the drought spatial distribution pattern. The drought characteristics extracted in Section 3.1.2 and the longitude and latitude of the corresponding meteorological stations were used as input variables for the K-means cluster model. These variables have different ranges and units, so they were normalized before being inputted into the K-means model to eliminate negative effects [5]. In general, the results of K-means depend largely on the initialization of centroids, and the method is less efficient in certain cases and easily falls to a local extreme value [45,46]. To eliminate these limitations, the revised method proposed by Zhuang et al. [47] was used in this study. In this revised method, an optimized selection of initial centroids is applied, and the information entropy theory is introduced when the unsupervised clustering algorithm is implemented. Compared with the traditional K-means algorithm, the revised method has a higher detection rate and a lower false alarm rate.

The K-means method is unsupervised, and the number of optimal  $k$  partitions or the optimal number of clusters needs to be determined. In this study, we utilized several quantitative measures to evaluate the cluster results and determine the optimal number of clusters. These quantitative measures include two R packages (Nbclust and Mclust) and two criteria (Elbow and Calinsky). Nbclust and Mclust provide 26 and 14 different indicators, respectively [48,49]. The number of indicators corresponding to the optimal number of clusters is greater. The Elbow standard calculates the sum of squared errors (SSE) to determine the number of clusters. As the number of clusters increases, SSE decreases accordingly; when the decline slows down, an inflection point arises, and the cluster value at the inflection point is used as the optimal number of clusters [50]. The Calinsky criterion evaluates the local optimal clustering number by calculating the SSE between groups and the SSE within a group. The smaller the SSE within a group is, the larger the SSE between groups is, and this result is reflected in the variance ratio criterion (VRC) value. A large VRC value indicates an optimal number of clusters [51].

Another task that should be performed when analyzing cluster results is to determine whether the drought characteristics from meteorological stations within a given partition are homogeneous or heterogeneous. The heterogeneity test [52] that compares the sample L-moment ratio with kappa distribution parameters can effectively deal with this matter. The heterogeneity statistic,  $H_i$ , can be calculated as follows [25]:

$$H_i = \frac{(V_i - \mu_{vi})}{\sigma_{vi}} \quad i = 1, 2, 3, \quad (4)$$

$$V_i = \sqrt{\left\{ \frac{\sum_{j=1}^N n_j (a-b)^2}{\sum_{j=1}^N n_j} \right\}} \quad i = 1, 2, 3, \quad (5)$$

where  $\mu_{vi}$  is the means of simulated  $V_i (i = 1, 2, 3)$  values,  $\sigma_{vi}$  is the standard deviations of simulated  $V_i (i = 1, 2, 3)$  values,  $a$  is the sample L-moment at each site,  $b$  is the average sample L-moments at a regional scale, and  $n_j$  is the length of the time series at site  $j$ . If  $H_i < 1 (i = 1, 2, 3)$ , then the region can be regarded as acceptably homogeneous. If  $1 < H_i < 2$ , then the region can be regarded as possibly homogeneous. If  $H_i > 2$ , then the region can be viewed as heterogeneous [4,37].

## 4. Results

### 4.1. Drought Characteristics and Their Spatial Distribution

We calculated the 1-, 3-, 6-, and 12-month SPEIs for Hunan Province from 1965 to 2015. Figure 4 displays the variability of the SPEI value with different time scales. Drought events had a shorter duration and higher intensity for 1-month SPEI than for 3-, 6-, and

12-month SPEI. This result indicates that an increase in time scale has a smoothing effect on the intensity and duration of a single drought [7]. For 6- and 12-month SPEI, the drought event with the highest intensity occurred in October 1998 (SPEI 6 =  $-2.146$ ) and January 2011 (SPEI 12 =  $-1.874$ ), respectively. This result means that drought characteristics vary with different drought time scales. Musei et al. [7] also observed this phenomenon.

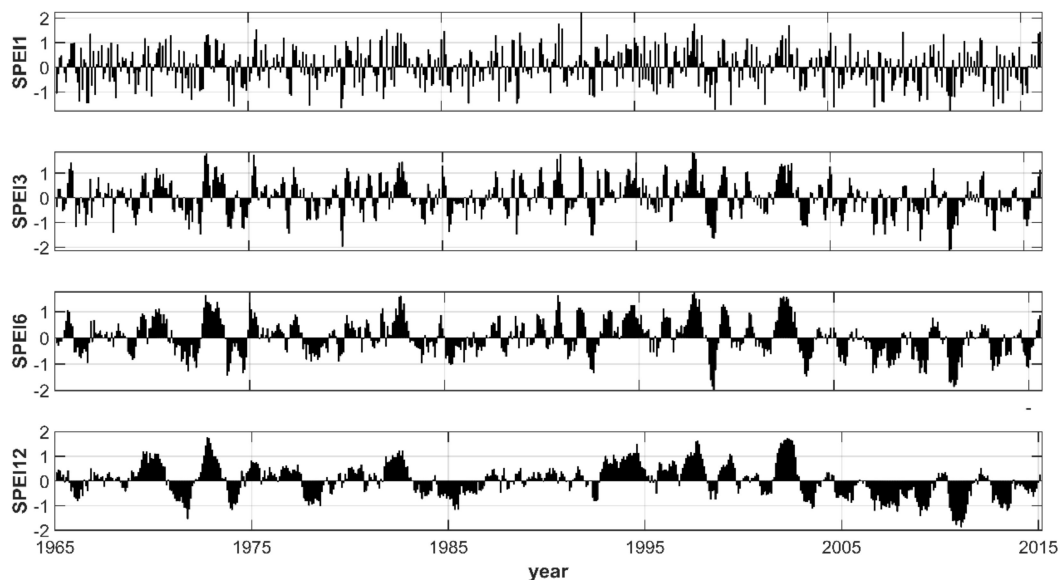


**Figure 4.** SPEI profiles with different time scales (SPEI–1, SPEI–3, SPEI–6, and SPEI–12).

In the past five decades, drought events that lasted for 10 months mostly began in summer and winter and lasted until the winter of the following year. According to the profile of SPEI-12 (Figure 4), from 1965 to 2015, Hunan Province experienced eight drought events that lasted more than 10 months; these events began in 1970, 1977, 1984, 2004, 2006, 2008, 2010, and 2012.

Drought duration (DD), drought severity (DS), and drought intensity (DI) were extracted from each station. A total of 7533 drought events were found throughout all stations, with an average of 85 drought events per station (accounting for 24.67–29.58%) with an average duration of 1.98 months and average severity of 2.25. Approximately, 21.6% of the stations had drought events that lasted more than 8 months; most drought events lasted less than six months. A single drought event at several stations was serious despite the weak intensity, which may be due to the shortening of the drought duration.

The drought characteristics extracted from each station were interpolated through the kriging method to explore their spatial distribution pattern, and the results are shown in Figure 5. Figure 5e,f shows remarkable variations in the total drought events (TDE) and total drought durations (TDD), respectively, in Hunan Province during 1965–2015. TDE and TDD had almost similar spatial distribution patterns. The northern (Changde and Zhangjiajie) and southern (Yongzhou) parts of Hunan are prone to be affected by long-lasting droughts, whereas the central parts have fewer droughts.

Average drought duration (ADD), average drought severity (ADS) and average drought intensity (ADI) are nearly uniformly distributed throughout the province, as shown in Figure 5a–c. The severity of drought in these areas ranges from moderate to severe. The north-western (Jishou and Huaihua) and central (Shaoyang and Hengyang) parts of Hunan Province constantly experience severe, long-lasting drought. However, the north-eastern region (Yiyang, Changde and Yueyang) of Hunan Province often experiences short-term drought. Amongst the areas, Loudi is the most prone to short-duration, intense drought.



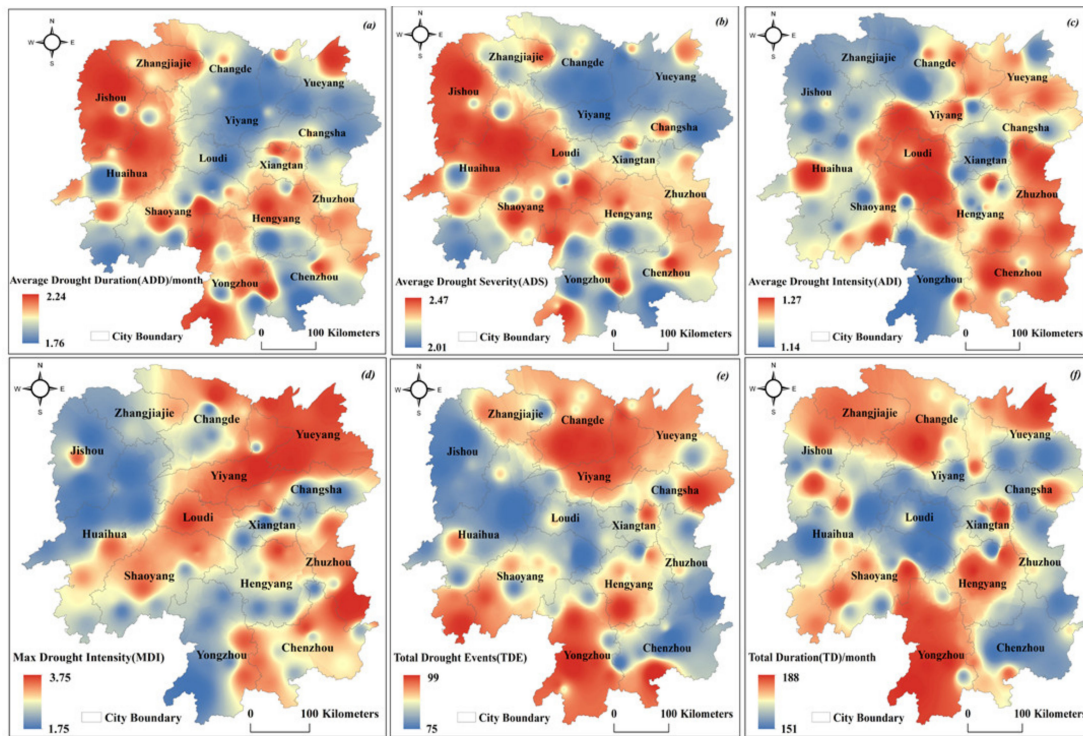


**Figure 5.** Spatial distribution of drought characteristics in Hunan: (a) ADD, (b) ADS, (c) ADI, (d) MDD, (e) TDE, and (f) TDD.

The spatial distribution of maximum drought intensity (MDI) also presented certain characteristics (Figure 5d). Only the most severe drought events at each station were explored in this work. The MDI in the north-,eastern part of Hunan is relatively strong, but the drought duration here is very short possibly because the area is prone to rapid drought, but it can rapidly recover from the drought.

Figure 6 shows the ADD, ADS, and ADI linear fits of all stations. Given that intensity is the accumulation of severity, with the extension of ADD time, drought turns to a wet state or returns to the normal state. Hence, ADD and ADS are positively correlated ( $R^2 = 0.76$ ), but ADD and ADI are negatively correlated ( $R^2 = 0.24$ ).

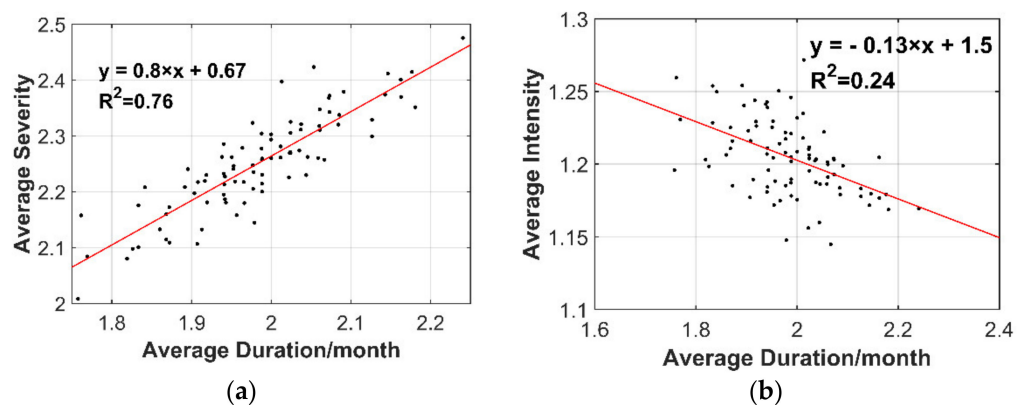


**Figure 6.** Correlation between (a) ADS and ADD and between (b) ADI and ADD at the meteorological stations.

## 4.2. Drought Spatial Distribution Pattern

### 4.2.1. Determining the Optimal Number of Clusters

The K-means clustering algorithm is highly efficient but choosing the optimal number of clusters is a tricky problem in this study. To determine the optimal number of clusters, different  $k$  values from 2 to 9 were used to partition meteorological stations, and the corresponding quantity evaluation measurements are shown in Table 3. All quantitative measures, except for the Calinsky criterion, indicate that 3 is the optimal number of clusters. In addition, the VRC values exhibit only slight differences between  $k = 3$  and  $k = 4$ , with corresponding values of 30.36 and 30.42, respectively. The drought characteristics heterogeneity test was conducted for all clusters, and the results showed that the drought characteristics for each cluster are homogeneous (Table 4). Hence, 3 is the optimal number of clusters for Hunan Province to partition these meteorological stations.

**Table 3.** Quantity evaluation measurements for different numbers of clusters.

Number of Clusters (k)	Nbclust (Number of Indicators)	Mclust (Number of Indicators)	Elbow Rule (SSE)	Calinsky Criterion (VRC)
2	4	NA	17.49	28.93
3	7	4	13.63	30.36
4	4	NA	11.20	30.42
5	1	3	9.57	29.91
6	NA	NA	8.56	28.4
7	NA	NA	7.68	27.57
8	NA	NA	6.87	27.45
9	NA	NA	6.12	27.82

**Table 4.** Heterogeneity test results for different clusters.

	Cluster 1			Cluster 2			Cluster 3		
	H(1)	H(2)	H(3)	H(1)	H(2)	H(3)	H(1)	H(2)	H(3)
DD	0.25	0.38	−0.47	0.46	−0.21	0.02	0.39	−0.13	0.42
DS	0.21	−0.25	0.39	0.37	−0.37	0.90	0.34	−0.07	−0.68
DI	0.39	−0.38	1.13	0.33	−0.16	−0.27	0.44	−0.02	−0.14
Latitude	0.47	−0.52	0.04	0.56	0.05	−1.06	0.17	−0.41	−0.83
Longitude	0.69	0.73	−0.13	0.34	−0.78	0.31	0.34	−0.50	−0.29

### 4.2.2. Drought Spatial Distribution Pattern for Clusters

The clusters of the meteorological stations are shown in Figure 7a, and they are divided into three clusters in terms of geography (Figure 7b) as per city boundaries. Cluster 1 includes most of the western meteorological stations, Cluster 2 includes the northeast stations, and Cluster 3 includes the southern stations. This clustering result is consistent with the division of the economic zones and landform types of Hunan [53]. Cluster 1 is located in undeveloped economic conditions where landforms are dominated by mountains and plateaus. Cluster 2 is in less-developed economic conditions where landforms are surrounded by mountains and plains. Cluster 3 is located in well-developed economic conditions where landforms are dominated by basins and hills.

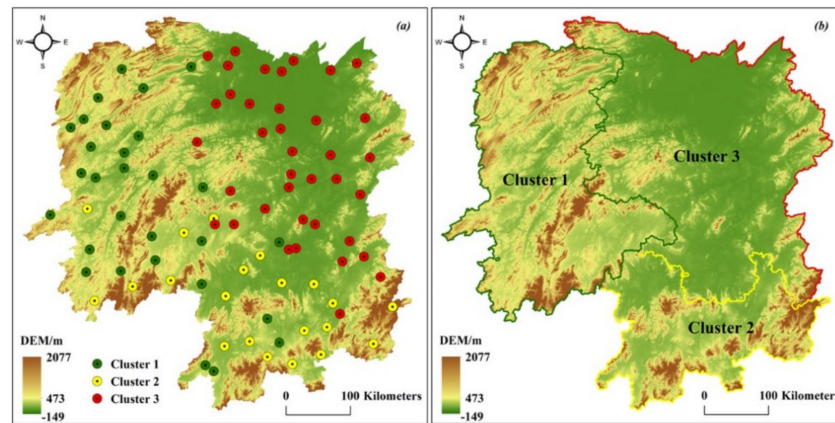


**Figure 7.** Regionalization of meteorological stations: (a) Spatial distribution of clustering stations and (b) division of arid space according to the clustering stations.

The investigation of the features of the centroid for each cluster shows that most of the drought events in Cluster 1 are slow droughts with low intensity and frequency. Cluster 2 has fast droughts with high intensity and frequency. Cluster 3 is highly susceptible to severe droughts. From the perspective of the features of ADD-ADS-ADI, the drought duration of Cluster 1 is long, but the intensity of each drought event is weak. Cluster 2 shows opposite drought characteristics relative to Cluster 1 (Figure 8a–c). The MDI value of Cluster 3 is large, which means that this area is prone to severe drought (Figure 8d). From the perspective of total drought duration and frequency, although Cluster 1 has the fewest drought events from 1965 to 2015, the duration of the events is the longest, whereas cluster 2 shows an opposite characteristic relative to Cluster 1 (Figure 8e,f).

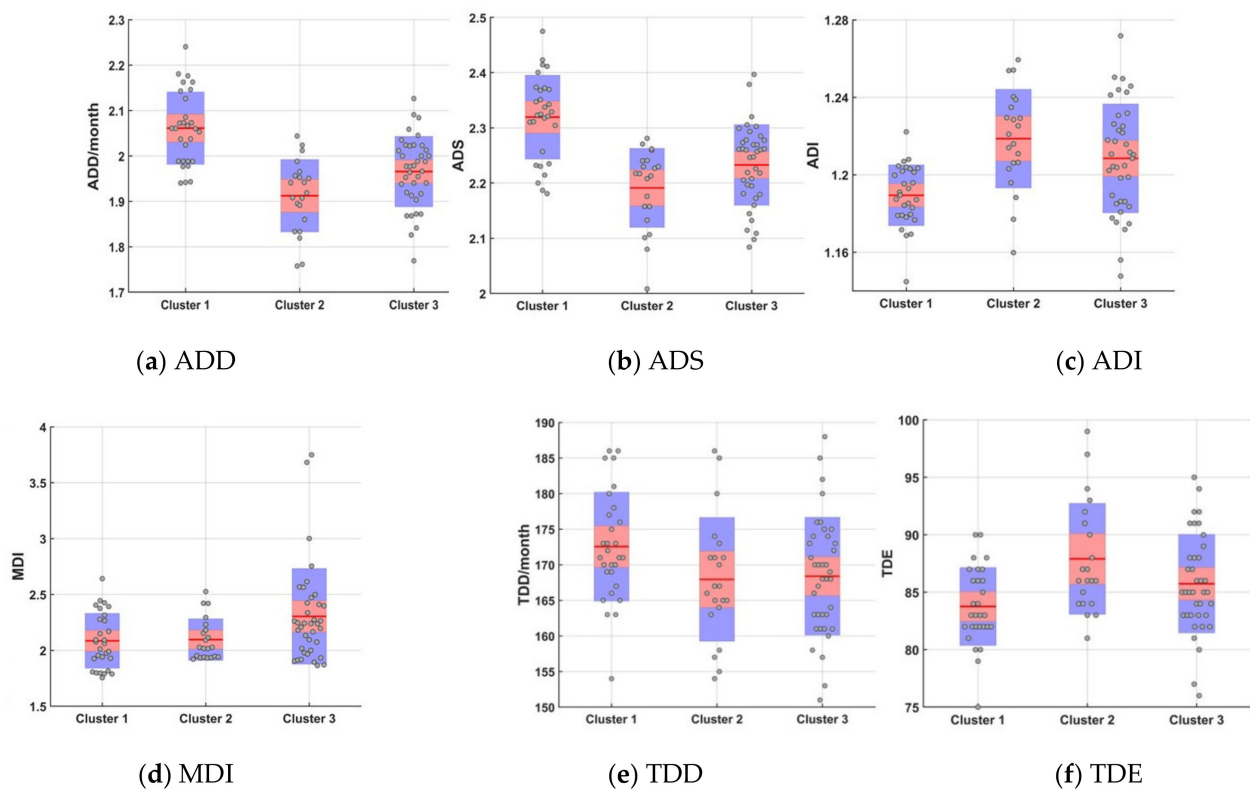


**Figure 8.** Box plot of station drought characteristics of the three clusters (average drought duration (a) (ADD), average drought severity (b) (ADS), average drought intensity (c) (ADI), max drought intensity (d) (MDI), total drought durations (e) (TDD), and total drought events (f) (TDE)).

To explore the differences in the dry/wet transitions of the three clusters at the same time, we calculated the time series values of the three clusters of SPEI-12. The differences in the status of drought transitions in the three periods were determined. The first was from August 1967 to June 1969; the dry/wet states of Clusters 1, 2, and 3 were continuous humidity, slightly wet to slightly dry, and slightly dry to slightly wet, respectively. The second was from December 1998 to August 1999, where the dry/wet states of Clusters 1, 2, and 3 were slightly dry, severely dry to slightly dry, and slightly wet, respectively. The third was from September 2009 to August 2011, where the dry/wet states of Clusters 1, 2, and 3 showed slight recovery, continuous drought, and wet-to-drought statuses, respectively. As shown in Table 5, Clusters 1 and 2 have opposite responses to drought. When a strong drought occurs, the recovery speed of Cluster 3 is the highest, followed by that of Cluster 1 and Cluster 2 (the slowest recovery).

**Table 5.** Three periods for the transition of the dry/wet status of the three clusters.

	Cluster 1	Cluster 2	Cluster 3
August 1967–June 1969	Continuous wet	Slightly wet to mildly dry	Mildly dry to slightly wet
December 1998–August 1999	Mildly dry	Severely dry	Slightly wet
September 2009–August 2011	Slight recovery	Continuous drought	Wet to drought

## 5. Discussion

The overall distribution of drought events in Hunan Province was determined by analyzing the SPEI-12 time series values of all stations (Figure 4). From 1965 to 2015, the province experienced eight drought events that lasted for more than 10 months (Figure 4). The interval between drought events from 1965 to 2000 was seven years (1970, 1977, and 1984), and the drought period decreased by two years from 2000 to 2015 (2004, 2006, 2008, 2010, and 2012). Zhang et al. [54] analyzed the drought in Hunan Province using the rotated empirical orthogonal function and discovered three main drought cycles, namely, 2, 7, and 18 years. The drought time distribution is mainly affected by the atmospheric circulation, in which two- to three-year periodic oscillation is related to the quasi-two-year oscillation (QBO) of the tropospheric atmospheric circulation, and the six-year cycle is related to the seven-year quasi-period of the five-year related ENSO event. On average, the drought at each station lasts for about two months, and summer and winter droughts are prone to occur. Zhang et al. [40] analyzed the annual and seasonal distributions of droughts in Hunan Province between 1989 and 2008. During this period, nine summer droughts, six winter droughts, and five spring and autumn droughts occurred, a result that is consistent with the conclusion of this study. This study proved this conclusion on a longer time scale. A possible reason Hunan Province is prone to summer drought is that it is affected by the Pacific subtropical high-pressure air mass. When the airflow does not go from south to north, a strong summer drought emerges, and this phenomenon occurs in the Yangtze River Basin. This condition once again proves the strong influence of atmospheric circulation on regional drought.

This study proposed an effective framework for dividing meteorological stations through an SPEI time series by using the K-means clustering method to analyze the spatial distribution characteristics of partial drought. The results showed that Hunan Province can be divided into three clusters. Cluster 1 stations are mainly distributed in the high-altitude areas of Hunan Province, and Cluster 2 stations are mainly distributed in southern Hunan. Cluster 3 stations are mainly distributed in basins and hilly areas and prone to severe drought. An interesting phenomenon is that Nanling Mountain serves as the dividing line between Clusters 1 and 2, which further proves the influence of topographical factors on drought [14]. Yang et al. [55] reported that in plateaus and mountainous areas with complex terrain, the order of drought spread varies with altitude. Agricultural droughts in high-altitude areas evolve into hydrological droughts. The opposite is true for low-altitude areas. Altitude plays a key role in the spread of drought in plateau areas. Wang et al. [56]

studied the spread of drought in 16 sub-basins of a river basin from 1980 to 2014, and the results showed that the topographic index and hydrological drought have a significant correlation. These experimental results show that topographical factors are important content in drought research whether in plateau or watershed areas. The impact of Hunan Province on drought due to its special topography is also obvious. The reason is manifested in two aspects: (1) The high altitude affects the distribution of airflow, which in turn affects precipitation. (2) The second aspect is directly affected by photosynthesis. Topography also indirectly influences vegetation types, and the drought-resistance capabilities of various vegetation types still differ [57]. All three clusters can be identified as severe droughts. However, for several drought events in similar specific periods, the dry/wet transition of each cluster is different (Table 5), which also proves the regional differences in the spatial distribution of drought in Hunan Province.

The effective zoning of drought in Hunan Province can allow the government to make powerful decisions on allocating water resources and preventing droughts. The north-western region of Hunan, Cluster 1, is prone to slow, low-intensity drought. This area is mainly the woodland area. Therefore, woodland species must be diversified to create a good ecological environment. The southern part of Hunan in cluster 2 is prone to rapid high-intensity drought, and preventive measures are difficult. Water conservancy project construction should be implemented properly. Dongting Lake and its four main rivers (Xiangjiang, Zishui, Yuanshui, and Lishui) should be introduced into the area to effectively solve the water supply problem. Cluster 3 has diversified vegetation and is prone to severe drought. Given the large area of arable land in this cluster, the planting structure needs to be rationally improved, and food security issues must be reduced.

We selected several drought characteristics extracted from SPEI through the operational theory for clustering. Results showed that Hunan Province is divided into three arid regions, each of which has similar characteristics. However, this study only performed clustering of drought characteristics. The regionalization of aridity is affected by airflow, topography, vegetation types, and human activities. These factors should be considered in the future.

The framework proposed in this study is flexible. For different regions, we can add other drought features. For example, wavelet analysis can be used to extract sites with similar frequency spectra for clustering. Considering the impact of terrain on drought, we can compare SWAT's DEM division results with drought feature division results via overlay analysis. Moreover, the main factors that affect drought can be extracted through principal component analysis then clustered. For the clustered results, we can use cross-wavelet analysis to compare the correlations between subregional drought and hydrology, vegetation, climate, and other variables to ensure the results are convincing.

## 6. Conclusions

The formation of drought is complex, diverse, and greatly affected by geographic locations. Understanding the regional nature of drought provides a strong foundation for spatial water resource management and planning. This study proposed a framework to explore spatiotemporal distribution patterns for achieving an improved understanding of drought events for a given area. When the framework was applied to Hunan Province, three clusters with different drought characteristics were found. The proposed framework is flexible because the parameters can be adjusted to obtain the best results for a given area, and it can provide feasible drought predictions for local decision-makers.

This study has the following limitations. Firstly, it considered only the spatiotemporal distribution characteristics of drought and did not include other influencing factors. For areas with highly complex terrain factors, the clustering may not be good. Secondly, for situations where meteorological stations have many historical deficiencies, the practicality of this method needs to be further studied. In future experiments, we should incorporate multiple features, such as terrain and trend features, when performing clustering to im-

prove the accuracy of clustering. Moreover, determining whether this clustering method can be used to predict future drought trends is another research step.

**Author Contributions:** Conceptualization, C.H., S.H., M.H.A.B. and Y.H.; methodology, C.H., S.H. and M.H.A.B. software, C.H. and S.H.; validation, C.H., S.H. and Y.H.; investigation, C.H. and Y.H.; resources, C.H. and S.H., data curation, C.H., S.H. and M.H.A.B.; writing—original draft preparation, C.H., S.H. and M.H.A.B.; writing—review and editing, C.H. and S.H.; visualization, C.H.; supervision, S.H.; project administration, S.H.; funding acquisition, S.H. All authors have read and agreed to the published version of the manuscript.

**Funding:** This research was funded by the Hunan Provincial Natural Science Foundation Project, grant number 2018JJ3348, Scientific Research Project of Hunan Provincial Department of Education, grant number 17C0952 and The Open Project of Hunan Provincial Key Laboratory of Remote Sensing Monitoring of Ecological Environment in Dongting Lake Region, grant number DTH Key Lab.2021.005.

**Conflicts of Interest:** The authors declare no conflict of interest.

## Abbreviations

PCI	Precipitation Condition Index
TCI	Temperature Condition Index
SPI	Standardized Precipitation Index
SPEI	Standardized Precipitation Evapotranspiration Index
PET	Potential Evapotranspiration
DD	Drought Duration
ADD	Average Drought Duration
DS	Drought Severity
ADS	Average Drought Severity
DI	Drought Intensity
ADI	Average Drought Intensity
MDI	Max Drought Intensity
TDE	Total Drought Events
TDD	Total Drought Durations
SSE	Sum of Squared Errors
VRC	Variance Ratio Criterion

## References

1. Soleimani Motlagh, M.; Ghasemieh, H.; Talebi, A.; Abdollahi, K. Identification and Analysis of Drought Propagation of Groundwater During Past and Future Periods. *Water Resour. Manag.* **2016**, *31*, 109–125. [[CrossRef](#)]
2. Shiau, J.-T.; Lin, J.-W. Clustering Quantile Regression-Based Drought Trends in Taiwan. *Water Resour. Manag.* **2015**, *30*, 1053–1069. [[CrossRef](#)]
3. Bae, S.; Lee, S.-H.; Yoo, S.-H.; Kim, T. Analysis of Drought Intensity and Trends Using the Modified SPEI in South Korea from 1981 to 2010. *Water* **2018**, *10*, 327. [[CrossRef](#)]
4. Abolverdi, J.; Khalili, D. Development of Regional Rainfall Annual Maxima for Southwestern Iran by L-Moments. *Water Resour Manag.* **2010**, *24*, 2501–2526. [[CrossRef](#)]
5. Goyal, M.K.; Sharma, A. A fuzzy c-means approach regionalization for analysis of meteorological drought homogeneous regions in western India. *Nat. Hazards* **2016**, *84*, 1831–1847. [[CrossRef](#)]
6. Sarle, W.S. Algorithms for Clustering Data. *Technometrics* **1990**, *32*, 227–229. [[CrossRef](#)]
7. Musei, S.K.; Nyaga, J.M.; Dubow, A.Z. SPEI-based spatial and temporal evaluation of drought in Somalia. *J. Arid Environ.* **2021**, *184*, 104296. [[CrossRef](#)]
8. Ghaderpour, E.; Vujadinovic, T.; Hassan, Q.K. Application of the Least-Squares Wavelet software in hydrology: Athabasca River Basin. *J. Hydrol. Reg. Stud.* **2021**, *36*, 100847. [[CrossRef](#)]
9. Gouveia, C.M.; Trigo, R.M.; Beguería, S.; Vicente-Serrano, S.M. Drought impacts on vegetation activity in the Mediterranean region: An assessment using remote sensing data and multi-scale drought indicators. *Glob. Planet. Chang.* **2017**, *151*, 15–27. [[CrossRef](#)]
10. Alizadeh, M.R.; Nikoo, M.R. A fusion-based methodology for meteorological drought estimation using remote sensing data. *Remote Sens. Environ.* **2018**, *211*, 229–247. [[CrossRef](#)]

11. West, H.; Quinn, N.; Horswell, M. Remote sensing for drought monitoring & impact assessment: Progress, past challenges and future opportunities. *Remote Sens. Environ.* **2019**, *232*, 111291. [[CrossRef](#)]
12. Liu, B.; Liang, M.; Huang, Z.; Tan, X. Duration–severity–area characteristics of drought events in eastern China determined using a three-dimensional clustering method. *Int. J. Climatol.* **2020**, *41*, E3065–E3084. [[CrossRef](#)]
13. Mohammed, W.E.; Algarni, S. A remote sensing study of spatiotemporal variations in drought conditions in northern Asir, Saudi Arabia. *Environ. Monit. Assess.* **2020**, *192*, 784. [[CrossRef](#)]
14. Agutu, N.O.; Awange, J.L.; Ndehedehe, C.; Mwaniki, M. Consistency of agricultural drought characterization over Upper Greater Horn of Africa (1982–2013): Topographical, gauge density, and model forcing influence. *Sci. Total Environ.* **2020**, *709*, 135149. [[CrossRef](#)]
15. Zhu, Q.; Luo, Y.; Zhou, D.; Xu, Y.-P.; Wang, G.; Tian, Y. Drought prediction using in situ and remote sensing products with SVM over the Xiang River Basin, China. *Nat. Hazards* **2020**, *105*, 2161–2185. [[CrossRef](#)]
16. Zhang, A.; Jia, G.; Wang, H. Improving meteorological drought monitoring capability over tropical and subtropical water-limited ecosystems: Evaluation and ensemble of the Microwave Integrated Drought Index. *Environ. Res. Lett.* **2019**, *14*, 044025. [[CrossRef](#)]
17. Dinku, T.; Ceccato, P.; Grover-Kopec, E.; Lemma, M.; Connor, S.J.; Ropelewski, C.F. Validation of satellite rainfall products over East Africa’s complex topography. *Int. J. Remote Sens.* **2007**, *28*, 1503–1526. [[CrossRef](#)]
18. Dinku, T.; Chidzambwa, S.; Ceccato, P.; Connor, S.J.; Ropelewski, C.F. Validation of high-resolution satellite rainfall products over complex terrain. *Int. J. Remote Sens.* **2008**, *29*, 4097–4110. [[CrossRef](#)]
19. Ezzine, H.; Bouziane, A.; Ouazar, D.; Hasnaoui, M.D. Downscaling of Open Coarse Precipitation Data through Spatial and Statistical Analysis, Integrating NDVI, NDWI, Elevation, and Distance from Sea. *Adv. Meteorol.* **2017**, *2017*, 20. [[CrossRef](#)]
20. Yang, X.; Sun, J.; Gao, J.; Qiao, S.; Zhang, B.; Bao, H.; Feng, X.; Wang, S. Effects of Climate Change on Cultivation Patterns and Climate Suitability of Spring Maize in Inner Mongolia. *Sustainability* **2021**, *13*, 8072. [[CrossRef](#)]
21. Yevjevich, V. An objective approach to definitions and investigations of continental hydrologic droughts. *J. Hydrol.* **1969**, *7*, 353. [[CrossRef](#)]
22. Pulighe, G.; Lupia, F.; Chen, H.; Yin, H. Modeling Climate Change Impacts on Water Balance of a Mediterranean Watershed Using SWAT+. *Hydrology* **2021**, *8*, 157. [[CrossRef](#)]
23. Brouziyne, Y.; Abouabdillah, A.; Chehbouni, A.; Hanich, L.; Bergaoui, K.; McDonnell, R.; Benaabidate, L. Assessing Hydrological Vulnerability to Future Droughts in a Mediterranean Watershed: Combined Indices-Based and Distributed Modeling Approaches. *Water* **2020**, *12*, 2333. [[CrossRef](#)]
24. Ghaderpour, E.; Ince, E.S.; Pagiatakis, S.D. Least-squares cross-wavelet analysis and its applications in geophysical time series. *J. Geod.* **2018**, *92*, 1223–1236. [[CrossRef](#)]
25. Zhang, Y.; Xie, P.; Pu, X.; Xia, F.; An, J.; Wang, P.; Mei, Q. Spatial and Temporal Variability of Drought and Precipitation Using Cluster Analysis in Xinjiang, Northwest China. *Asia-Pac. J. Atmos. Sci.* **2018**, *55*, 155–164. [[CrossRef](#)]
26. Oliver, J.E. Monthly precipitation distribution: A comparative index. *Prof. Geogr.* **1980**, *32*, 300–309. [[CrossRef](#)]
27. Kogan, N.F. Droughts of the Late 1980s in the United States as Derived from NOAA Polar-Orbiting Satellite Data. *Bull. Am. Meteorol. Soc.* **1995**, *76*, 655–668. [[CrossRef](#)]
28. McKee, T.; Doesken, N.; Kleist, J. The Relationship of Drought Frequency and Duration to Time Scales. In Proceedings of the 8th Conference on Applied Climatology, Zurich, Switzerland, 13–17 September 2010; American Meteorological Society: Boston, MA, USA, 1993; pp. 179–183.
29. Vicente-Serrano, S.M.; Beguería, S.; López-Moreno, J.I. A Multiscalar Drought Index Sensitive to Global Warming: The Standardized Precipitation Evapotranspiration Index. *J. Clim.* **2010**, *23*, 1696–1718. [[CrossRef](#)]
30. Richard, R.; Heim, J. A Review of Twentieth-Century Drought Indices Used in the United States. *Bull. Am. Meteorol. Soc.* **2002**, *83*, 1149–1166.
31. He, J.; Yang, X.; Li, Z.; Zhang, X.; Tang, Q. Spatiotemporal Variations of Meteorological Droughts in China During 1961–2014: An Investigation Based on Multi-Threshold Identification. *Int. J. Disaster Risk Sci.* **2016**, *7*, 63–76. [[CrossRef](#)]
32. Sun, Z.; Zhang, J.; Yan, D.; Wu, L.; Guo, E. The impact of irrigation water supply rate on agricultural drought disaster risk: A case about maize based on EPIC in Baicheng City, China. *Nat. Hazards* **2015**, *78*, 23–40. [[CrossRef](#)]
33. Malik, A.; Kumar, A.; Kisi, O.; Khan, N.; Salih, S.Q.; Yaseen, Z.M. Analysis of dry and wet climate characteristics at Uttarakhand (India) using effective drought index. *Nat. Hazards* **2021**, *105*, 1643–1662. [[CrossRef](#)]
34. Dracup, J.A.; Lee, K.S.; Paulson, E.G. On the statistical characteristics of drought events. *Water Resour. Res.* **1980**, *16*, 289–296. [[CrossRef](#)]
35. Wang, L.; Zhang, X.; Wang, S.; Salahou, M.K.; Fang, Y. Analysis and Application of Drought Characteristics Based on Theory of Runs and Copulas in Yunnan, Southwest China. *Int. J. Environ. Res. Public Health* **2020**, *17*, 4654. [[CrossRef](#)] [[PubMed](#)]
36. Bloomfield, J.P.; Marchant, B.P.; Bricker, S.H.; Morgan, R.B. Regional analysis of groundwater droughts using hydrograph classification. *Hydrol. Earth Syst. Sci.* **2015**, *19*, 4327–4344. [[CrossRef](#)]
37. Xie, P.; Lei, X.; Zhang, Y.; Wang, M.; Han, I.; Chen, Q. Cluster analysis of drought variation and its mutation characteristics in Xinjiang province, during 1961–2015. *Hydrol. Res.* **2018**, *49*, 1016–1027. [[CrossRef](#)]
38. Ali, Z.; Hussain, I.; Faisal, M.; Shoukry, A.M.; Gani, S.; Ahmad, I. A framework to identify homogeneous drought characterization regions. *Theor. Appl. Climatol.* **2019**, *137*, 3161–3172. [[CrossRef](#)]

39. Du, J.; Fang, J.; Xu, W.; Shi, P. Analysis of dry/wet conditions using the standardized precipitation index and its potential usefulness for drought/flood monitoring in Hunan Province, China. *Stoch. Environ. Res. Risk Assess.* **2012**, *27*, 377–387. [[CrossRef](#)]
40. Zhang, Y.; Wang, J.; Shen, Z.; Xie, X. Evolution Characteristics of Seasonal Drought in Hunan Based on the Standardized Precipitation Index (SPI). *Geosci. Remote Sens.* **2019**, *2*, 56–64. [[CrossRef](#)]
41. Liu, Q.; Li, M.; Duan, J.; Wu, H. The Spatio-temporal Variation of Benefit of Cultivated Land Use based on GIS Technology in Hunan Province. *Econ. Geogr.* **2013**, *33*, 142–147. [[CrossRef](#)]
42. Vicente-Serrano, S.M.; Beguería, S.; López-Moreno, J.I.; Angulo, M.; El Kenawy, A. A New Global 0.5° Gridded Dataset (1901–2006) of a Multiscalar Drought Index: Comparison with Current Drought Index Datasets Based on the Palmer Drought Severity Index. *J. Hydrometeorol.* **2010**, *11*, 1033–1043. [[CrossRef](#)]
43. Thornthwaite, C.W. An Approach Toward a Rational Classification of Climate. *Soil Sci.* **1948**, *66*, 55–94. [[CrossRef](#)]
44. Wu, R.; Zhang, J.; Bao, Y.; Guo, E. Run Theory and Copula-Based Drought Risk Analysis for Songnen Grassland in Northeastern China. *Sustainability* **2019**, *11*, 6032. [[CrossRef](#)]
45. Celebi, M.E.; Kingravi, H.A.; Vela, P.A. A comparative study of efficient initialization methods for the k-means clustering algorithm. *Expert Syst. Appl.* **2013**, *40*, 200–210. [[CrossRef](#)]
46. Zhou, Z. *Machine Learning*; Tsinghua University Press: Beijing, China, 2016; p. 425.
47. Zhuang, C.; Cheng, L. Improved K- Means Algorithm Using in Anomaly Detection. *J. Chongqing Univ. Technol. (Nat. Sci.)* **2015**, *29*, 66–70.
48. Scrucca, L.; Fop, M.; Murphy, T.B.; Raftery, A.E. mclust 5: Clustering, Classification and Density Estimation Using Gaussian Finite Mixture Models. *R J.* **2016**, *8*, 289–317. [[CrossRef](#)]
49. Charrad, M.; Ghazzali, N.; Boiteau, V.; Niknafs, A. NbClust: An R Package for Determining the Relevant Number of Clusters in a Data Set. *J. Stat. Softw.* **2014**, *61*, 1–36. [[CrossRef](#)]
50. Chikumbo, O.; Granville, V. Optimal Clustering and Cluster Identity in Understanding High-Dimensional Data Spaces with Tightly Distributed Points. *Mach. Learn. Knowl. Extr.* **2019**, *1*, 715–744. [[CrossRef](#)]
51. Calinski, T.; Harabasz, J. A dendrite method for cluster analysis. *Commun. Stat. Theory Methods* **1974**, *3*, 1–27. [[CrossRef](#)]
52. Hosking, J.R.M.; Wallis, J.R. *Regional Frequency Analysis: An Approach Based on L-Moments*; Cambridge University Press: New York, NY, USA, 1997.
53. Zhu, X. *Hunan Geography*; Beijing Normal University Press: Beijing, China, 2014; p. 197.
54. Zhang, J.; Zhang, X.; Li, Z.; Zhang, J.; Xiao, Y.; Liu, Y.; Zhou, W. Spatial distribution and variation tendency of droughts and floods in Hunan province during the past 36 years. *J. Trop. Meteorol.* **2011**, *17*, 385–392. [[CrossRef](#)]
55. Yang, F.; Duan, X.; Guo, Q.; Lu, S.; Hsu, K. The spatiotemporal variations and propagation of droughts in Plateau Mountains of China. *Sci. Total Environ.* **2021**, *805*, 150257. [[CrossRef](#)] [[PubMed](#)]
56. Wang, J.; Wang, W.; Cheng, H.; Wang, H.; Zhu, Y. Propagation from Meteorological to Hydrological Drought and Its Influencing Factors in the Huaihe River Basin. *Water* **2021**, *13*, 1985. [[CrossRef](#)]
57. Schwartz, N.B.; Budsock, A.M.; Uriarte, M. Fragmentation, forest structure, and topography modulate impacts of drought in a tropical forest landscape. *Ecology* **2019**, *100*, e02677. [[CrossRef](#)] [[PubMed](#)]



Reproduced with permission of copyright owner. Further reproduction prohibited without permission.